

# Hsp90 chaperones PPAR $\gamma$ and regulates differentiation and survival of 3T3-L1 adipocytes

MT Nguyen<sup>1</sup>, P Csermely<sup>1</sup> and C Söti<sup>\*,1</sup>

Adipose tissue dysregulation has a major role in various human diseases. The peroxisome proliferator-activated receptor- $\gamma$  (PPAR $\gamma$ ) is a key regulator of adipocyte differentiation and function, as well as a target of insulin-sensitizing drugs. The Hsp90 chaperone stabilizes a diverse set of signaling 'client' proteins, thereby regulates various biological processes. Here we report a novel role for Hsp90 in controlling PPAR $\gamma$  stability and cellular differentiation. Specifically, we show that the Hsp90 inhibitors geldanamycin and novobiocin efficiently impede the differentiation of murine 3T3-L1 preadipocytes. Geldanamycin at higher concentrations also inhibits the survival of both developing and mature adipocytes, respectively. Further, Hsp90 inhibition disrupts an Hsp90-PPAR $\gamma$  complex, leads to the destabilization and proteasomal degradation of PPAR $\gamma$ , and inhibits the expression of PPAR $\gamma$  target genes, identifying PPAR $\gamma$  as an Hsp90 client. A similar destabilization of PPAR $\gamma$  and a halt of adipogenesis also occur in response to protein denaturing stresses caused by a single transient heat-shock or proteasome inhibition. Recovery from stress restores PPAR $\gamma$  stability and adipocyte differentiation. Thus, our findings reveal Hsp90 as a critical stress-responsive regulator of adipocyte biology and offer a potential therapeutic target in obesity and the metabolic syndrome.

*Cell Death and Differentiation* (2013) 20, 1654–1663; doi:10.1038/cdd.2013.129; published online 4 October 2013

White adipose tissue is an active metabolic endocrine organ that imparts on whole-body homeostasis. Adipose tissue expansion (obesity) and a consequent dysregulation have a prominent role in various systemic diseases including the metabolic syndrome.<sup>1,2</sup> The nuclear transcription factor, peroxisome proliferator-activated receptor  $\gamma$  (PPAR $\gamma$ ), emerged as a prime regulator of adipocyte biology.<sup>3,4</sup> PPAR $\gamma$  belongs to the RXR-heterodimeric group 1 of the nuclear receptor superfamily (NR1C3). Of its two major isoforms, PPAR $\gamma$ 1 is expressed in a variety of tissues, including the liver, skeletal muscle, macrophages, adipose tissue and bone. PPAR $\gamma$ 2 possesses a 30-amino-acid extension at its extreme N-terminus, and exclusively occurs in adipogenic cells.<sup>4</sup>

General and adipose-specific deletion of PPAR $\gamma$  in mice<sup>5–7</sup> and dominant-negative PPAR $\gamma$  mutations in humans<sup>8</sup> lead to lipodystrophy and severe insulin resistance. PPAR $\gamma$  activation by the antidiabetic thiazolidinediones as well as by adipocyte-targeted transgene expression of PPAR $\gamma$ 2 improves insulin sensitivity, adipokine and inflammatory profiles.<sup>9</sup> Similarly, human studies showed that a Pro12Ala variant of PPAR $\gamma$ 2 confers protection from weight gain and diabetes mellitus.<sup>10</sup> Consistently, PPAR $\gamma$  2 as well as its Pro12Ala variant contribute to longevity in mice.<sup>11,12</sup> The above examples show a profound impact of optimal adipose PPAR $\gamma$  function on systemic physiology and healthspan.

In response to adipogenic signals, parallel activation of the CCAAT/enhancer-binding proteins (C/EBP)  $\beta$  and  $\delta$  induces a mitotic clonal expansion (i.e., several rounds of postconfluent mitosis) of preadipocytes, as well as a marked transcriptional induction of PPAR $\gamma$  and C/EBP $\alpha$ .<sup>4,13</sup> Although PPAR $\gamma$  works in concert with C/EBP $\alpha$ , PPAR $\gamma$  is necessary and sufficient for adipogenesis. PPAR $\gamma$ -deficient embryonic stem cells are unable to differentiate into adipocytes,<sup>14,15</sup> whereas ectopic expression of PPAR $\gamma$  in mouse embryonic fibroblasts drives adipogenesis in the absence of C/EBP $\alpha$ .<sup>16</sup> Once activated by natural lipid derivatives, PPAR $\gamma$  heterodimerizes with RXR and regulates the transcription of hundreds of genes leading to terminal differentiation.<sup>17</sup> Besides, PPAR $\gamma$  is also indispensable for both function and survival of mature adipocytes.<sup>18,19</sup> An intricate regulation of PPAR $\gamma$  function also involves post-translational mechanisms including sumoylation and ubiquitin-dependent proteasomal degradation,<sup>20–22</sup> but is not fully understood.

Heat-shock protein 90 (Hsp90) is an evolutionarily conserved molecular chaperone essential for the folding and activity of several hundred thermodynamically unstable 'client' proteins, mainly kinases and nuclear receptors involved in cellular signaling, proliferation and cell survival.<sup>23–25</sup> (For a complete list of clients, see: [www.picard.ch/downloads/Hsp90interactors.pdf](http://www.picard.ch/downloads/Hsp90interactors.pdf).) Besides a uniform Hsp90 dependence

<sup>1</sup>Department of Medical Chemistry, Semmelweis University, Budapest, Hungary

\*Corresponding author: C Söti, Department of Medical Chemistry, Semmelweis University, PO Box 260, Budapest H-1444, Hungary. Tel: +36 1 4591500, extn. 60130; Fax: +36 1 4591500, extn. 60141; E-mail: [soti.csaba@med.semmelweis-univ.hu](mailto:soti.csaba@med.semmelweis-univ.hu)

**Keywords:** adipogenesis; diabetes; obesity; proteostasis; stress

**Abbreviations:** 3T3-L1, murine preadipocytic line derived from NIH-3T3 fibroblasts; Akt, protein kinase B; aP2, adipocyte protein 2; ADP, adenosine-5'-diphosphate; ATCC, American Type Culture Collection; ATP, adenosine-5'-triphosphate; C/EBP  $\beta$  and  $\delta$ , CCAAT/enhancer-binding proteins  $\beta$  and  $\delta$ ; Cdc2, cyclin-dependent kinase 1; DMSO, dimethyl sulfoxide; DTT, dithiothreitol; GA, geldanamycin; GLUT4, glucose transporter type 4; HepG2, human hepatoma cell line; HSF, heat-shock transcription factor; Hsp90, heat-shock protein 90; IC50, half maximal inhibitory concentration; IGF1, insulin-like growth factor 1; IP, immunoprecipitation; NP40, Nonidet P-40; NR, nuclear receptor superfamily; PBS, phosphate-buffered saline; PI3K, phosphatidylinositol-3-kinase; PPAR $\gamma$ , peroxisome proliferator-activated receptor- $\gamma$ ; qRT-PCR, real-time reverse-transcription PCR; RXR, retinoid X receptor; TGF $\beta$ , transforming growth factor  $\beta$ ; WB, western blot; Wnt, wingless-related integration-1

Received 16.1.13; revised 24.7.13; accepted 21.8.13; Edited by M Piacentini; published online 04.10.13

of NR3 steroid receptors, NR1 members exhibit a variable degree of reliance on Hsp90 from full dependence (aryl-hydrocarbon receptor) through absolute independence (thyroid receptor).<sup>23,26,27</sup> An earlier study found that all PPARs associated with bacterially expressed Hsp90 *in vitro*.<sup>28</sup> However, contrary to the predominantly supportive Hsp90-client interactions, Hsp90 was not required for PPAR $\alpha$  stability, repressed PPAR $\alpha$  and PPAR $\beta$  reporter activity, whereas did not significantly affect a PPAR $\gamma$ -dependent reporter. This example illustrates the individuality of Hsp90 interactions even among highly similar PPAR relatives. Moreover, the role of Hsp90 in PPAR $\gamma$  function remained unexplored.

Hsp90 occurs in two homologous and functionally redundant isoforms: in contrast to the more constitutive and ubiquitous Hsp90 $\beta$ , Hsp90 $\alpha$  exhibits a more stress-inducible and rather tissue-specific expression.<sup>24</sup> The chaperone cycle of Hsp90 is coordinated by ATP-binding and hydrolysis and involves a dynamic association of co-chaperones.<sup>23</sup> The N-terminal nucleotide antagonist geldanamycin (GA),<sup>29</sup> and other Hsp90 inhibitors disrupt the ATPase/chaperone cycle and destabilize diverse clients, offering a single-hit $\rightarrow$ multi-target type anticancer treatment.<sup>30</sup> Hsp90 also regulates the heat-shock response by releasing the heat-shock transcription factor HSF1 upon binding to denatured proteins.<sup>31</sup> However, the impact of proteostasis on Hsp90-client interactions remained elusive. Despite the increased awareness of the role of the heat-shock response in metabolic stress and obesity,<sup>32</sup> the involvement of Hsp90 in these conditions is, yet, similarly unclear. In this study, we investigate how Hsp90 and proteotoxic stress regulate adipogenesis and delineate the potential molecular mechanisms involved.

## Results

**Hsp90 inhibition impedes differentiation and survival of 3T3-L1 preadipocytes.** To investigate how Hsp90 modulates adipogenesis, mouse 3T3-L1 preadipocytes, a widely used experimental model was employed.<sup>33</sup> In response to hormonal stimulation, 3T3-L1 cells terminally differentiate into mature adipocytes in 2 weeks (Figure 1a) and accumulate triglycerides in lipid droplets, readily stained by Oil Red O (Figure 1b). A transient treatment of preadipocytes at the terminal differentiation phase by the Hsp90-specific N-terminal inhibitor geldanamycin (GA) efficiently suppressed adipogenesis in a concentration-dependent manner (Figures 1b and c). A similar inhibitory effect was obtained using the C-terminal Hsp90 inhibitor, novobiocin<sup>34</sup> (Supplementary Figure S1). Thus, various forms of Hsp90 inhibition compromised the terminal differentiation of 3T3-L1 cells.

Hsp90 inhibition might prevent differentiation through inducing cell death. However, we observed a large number of viable undifferentiated preadipocytes in response to either Hsp90 inhibitor (see the attached, unstained, elongated cells in Figure 1b and Supplementary Figure S1a). Therefore, we quantitatively analyzed both differentiation and viability from parallel GA-treated samples on day 14. Consistent with Hsp90's role in cell survival, GA induced extensive cell death, especially at higher concentrations. However, GA progressively compromised differentiation exceeding an over

80% inhibition at 56 nM without a significant effect on viability. Moreover, kinetic analysis revealed a 10-fold lower IC<sub>50</sub> value of GA on differentiation compared with that on survival (16.38 *versus* 163.6 nM), which was virtually unaffected by normalization to viability (Figure 1c and Supplementary Table S1). These results suggest that the differentiation-promoting effect of Hsp90 is a consequence of other than its pro-survival mechanism(s).

**Hsp90 inhibition depletes PPAR $\gamma$  protein levels.** Next, we investigated potential molecular mechanisms behind the GA-induced inhibition of adipogenesis. PPAR $\gamma$  is a master transcriptional regulator of adipocyte differentiation, acting in the terminal differentiation phase.<sup>4,17</sup> Indeed, we observed a robust induction of PPAR $\gamma$ 1 protein during adipocyte differentiation, starting from day 2 with a shift in favor of the adipose-specific PPAR $\gamma$ 2 later (Supplementary Figures S2a and b). Importantly, an overnight GA treatment entirely depleted both PPAR $\gamma$ 1 and 2 protein levels with IC<sub>50</sub> values of 51.0 and 40.8 nM, respectively (Figures 2a and b; Supplementary Table S1). Besides the abundant, modestly inducible Hsp90 $\beta$ , Hsp90 $\alpha$  was only detected in response to strong proteotoxic insults and remained at the detection limit in GA-treated 3T3-L1 cells (Figure 2a; Supplementary Figures S2a–d). These findings do not exclude a PPAR $\gamma$ -Hsp90 $\alpha$  interaction, but suggest that both PPAR $\gamma$  isoforms are predominantly chaperoned by Hsp90 $\beta$  in 3T3-L1 cells. GA under these conditions partially decreased the protein level of Akt, a known Hsp90 client,<sup>35</sup> which has a key role in insulin/IGF1-signaling acting downstream of phosphatidylinositol-3-kinase, a potent activator of adipogenesis<sup>9,36</sup> (Figures 2a and b). Accordingly, overnight treatment of 3T3-L1 cells with pharmacologic doses of the specific PI3K inhibitor LY294002 partially compromised adipogenesis (Supplementary Figures S3a and b). Hence, inhibition of the PI3K/Akt pathway by GA may contribute to the inhibition of 3T3-L1 differentiation. GA did not affect the level of the PPAR $\gamma$  cooperator, C/EBP $\alpha$  p42, which is consistent with an intact signaling/transcriptional function leading to terminal differentiation (Figure 2a). GA treatment also decreased PPAR $\gamma$  protein levels in HepG2 human hepatocytes (Supplementary Figure S4). Moreover, novobiocin depleted PPAR $\gamma$  in 3T3-L1 cells (Figure 2c). Thus, Hsp90 stabilizes PPAR $\gamma$  protein in mammalian cells.

## Inhibition of the Hsp90-PPAR $\gamma$ interaction triggers destabilization and proteasomal degradation of PPAR $\gamma$ .

To address whether PPAR $\gamma$  and Hsp90 physically interact, we immunoprecipitated endogenous PPAR $\gamma$  protein from 3T3-L1 adipocytes. Hsp90 was detected in a physical complex with PPAR $\gamma$ , which was disrupted by a 2-h GA treatment (Figure 3a). PPAR $\gamma$  is subject to proteasome-mediated turnover.<sup>20,21</sup> Prompted by these findings, we asked whether PPAR $\gamma$  might misfold and undergo proteasomal degradation in response to Hsp90 inhibition. Indeed, GA caused the complete disappearance of PPAR $\gamma$  from both the detergent soluble supernatant and insoluble pellet fractions of 3T3-L1 cell lysates (Figure 3b). A parallel treatment by the proteasome inhibitor MG132 induced the accumulation of both PPAR $\gamma$  and Akt in the detergent-insoluble pellet,

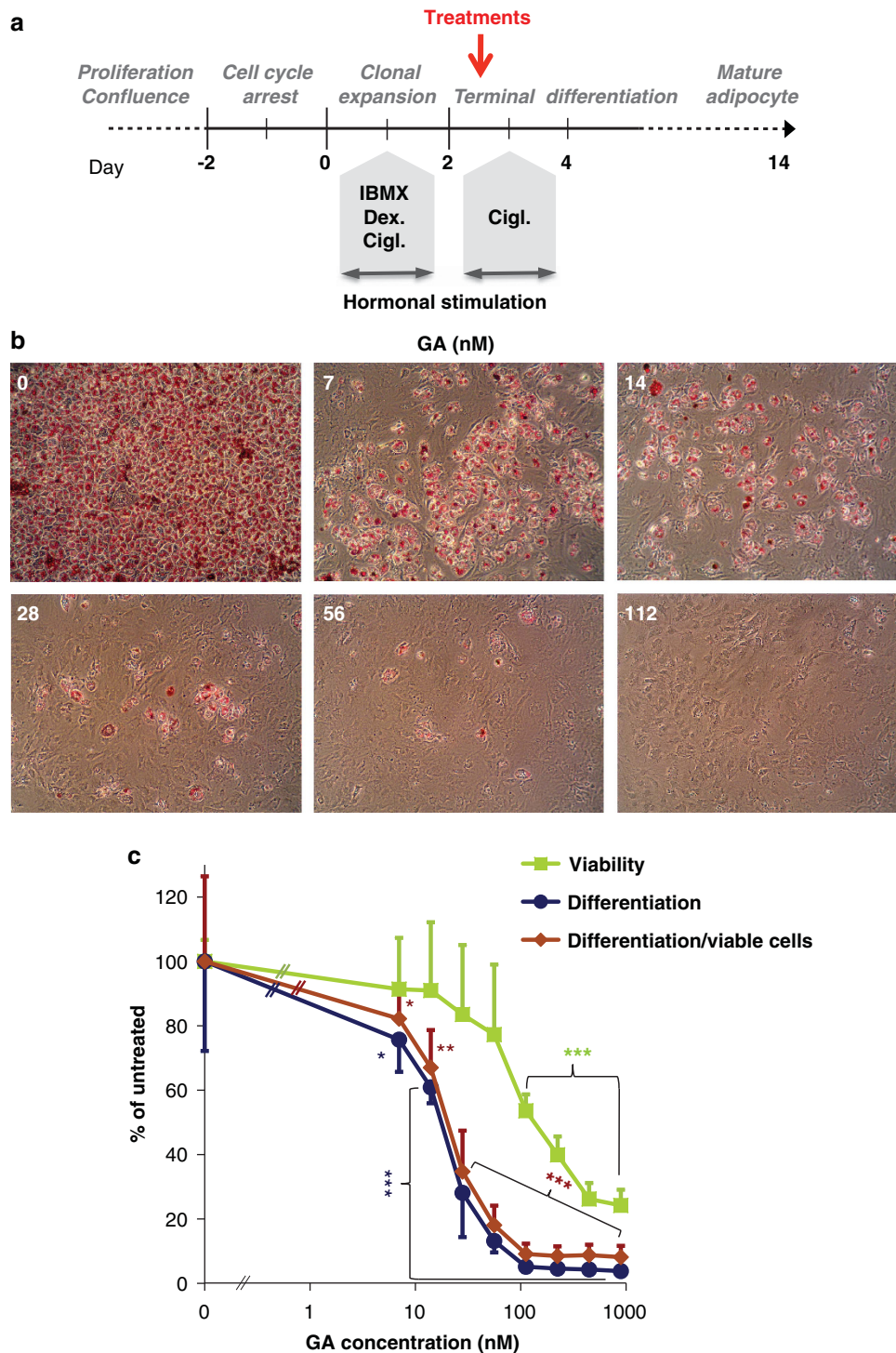


**Figure 1** Geldanamycin inhibits adipocyte differentiation in a concentration-dependent manner. (a) Timescale of 3T3-L1 preadipocyte differentiation. Stages, stimulation (by IBMX, dexamethasone, ciglitizone) and the time point of treatments on day 3 are indicated. (b) Oil Red O staining of 3T3-L1 cells on day 14, treated by various concentrations of geldanamycin (GA) for 20 h on day 3. Note the presence of unstained undifferentiated attached preadipocytes in GA-treated samples. Images are representatives of six independent experiments. (c) Parallel quantification of Oil Red O absorption by photometry and cell viability by trypan blue exclusion on day 14. Differentiation/viable cells is expressed by normalizing Oil Red O incorporation to viability. Values are means  $\pm$  S.D. of three experiments and statistically compared with the respective untreated controls. IC<sub>50</sub> values are compared in Supplementary Table S1. \* $P < 0.05$ , \*\* $P < 0.01$ , \*\*\* $P < 0.001$  by two-tailed unpaired t-test

demonstrating a destabilization-induced aggregation of PPAR $\gamma$ .

The timescale of GA treatment indicated a fast kinetics of PPAR $\gamma$  depletion (Figure 3c). Use of the translation inhibitor,

cycloheximide revealed a rapid turnover of PPAR $\gamma$  within 4 h (Figure 3c), in agreement with the robust expression, and proteasomal degradation of activated PPAR $\gamma$ .<sup>21</sup> Altogether, these results demonstrate that an association with Hsp90 is



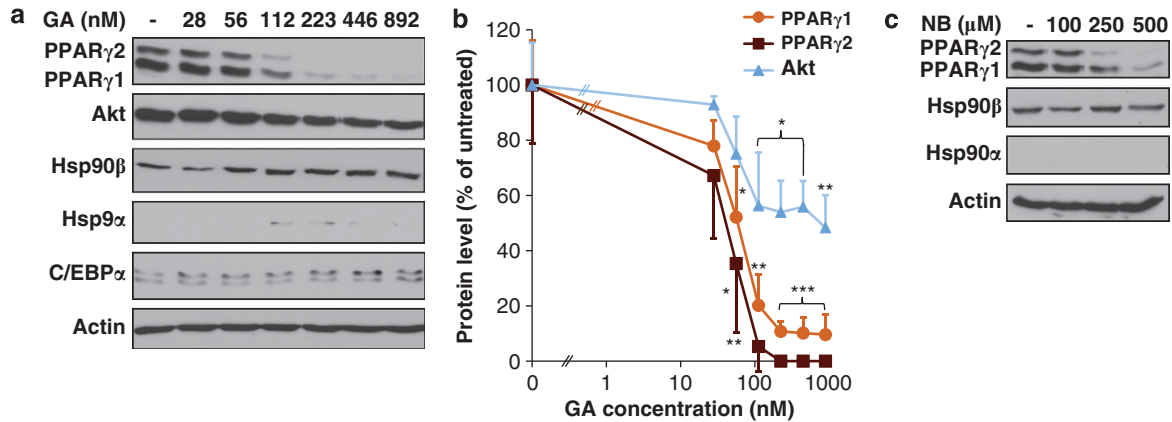


**Figure 2** Hsp90 inhibition depletes PPAR $\gamma$  protein in 3T3-L1 cells. (a) Effect of GA on PPAR $\gamma$ , Akt, Hsp90 $\alpha$ , Hsp90 $\beta$  and C/EBP $\alpha$  p42 protein levels. Western blots of lysates from 3T3-L1 cells treated by GA for 20 h on day 3. Images are representatives of three experiments. (b) Quantification of protein levels from the experiment shown in panel (a). Values are means  $\pm$  S.D. of three experiments and were statistically compared with the respective untreated controls. IC50 values are compared in Supplementary Table S1. \* $P < 0.05$ , \*\* $P < 0.01$ , \*\*\* $P < 0.001$  by two-tailed unpaired *t*-test. (c) Effect of novobiocin (NB) 3 on PPAR $\gamma$ , Hsp90 $\alpha$  and Hsp90 $\beta$  protein levels. Western blots of lysates from 3T3-L1 cells treated with NB for 20 h on day 3. Images are representatives of two experiments

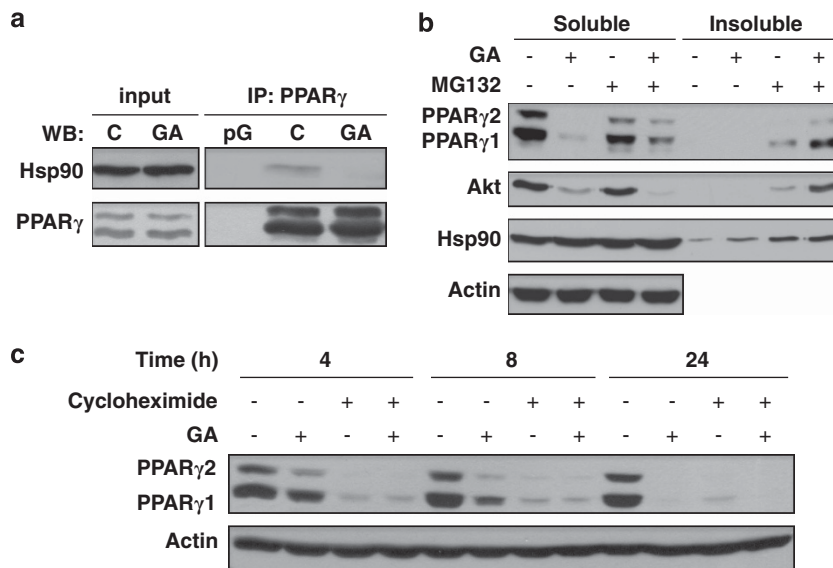


**Figure 3** Inhibition of the Hsp90-PPAR $\gamma$  interaction triggers destabilization and proteasomal degradation of PPAR $\gamma$ . (a) PPAR $\gamma$  physically interacts with Hsp90 in a GA-sensitive manner. Western blots showing the coprecipitation of Hsp90 with PPAR $\gamma$  from 3T3-L1 cells treated by 446 nM (0.25  $\mu$ g/ml) GA or vehicle for 2 h. pG, protein G control; C, control (DMSO vehicle). (b) GA induces misfolding and proteasomal degradation of PPAR $\gamma$ . Western blots of detergent soluble and insoluble lysates from cells treated by 446 nM GA and/or 20  $\mu$ M MG132 or DMSO vehicle for 24 h. (c) Timescale of GA and/or cycloheximide treatments on PPAR $\gamma$  protein levels. Western blots of protein lysates from cells treated by 446 nM GA and/or 25  $\mu$ g/ml cycloheximide or DMSO vehicle for 4, 8 or 24 h. Images are representatives of three experiments

indispensable for proper PPAR $\gamma$  folding and define PPAR $\gamma$  as an Hsp90 client protein.

**Hsp90 function is required for PPAR $\gamma$  transcriptional output and for survival of mature adipocytes.** Next, we investigated how Hsp90 inhibition affects PPAR $\gamma$ -driven downstream events. GA treatment prevented the induction of PPAR $\gamma$ -dependent target mRNAs important for autonomous (GLUT4, aP2) and for systemic (adiponectin) functions of adipocytes (Figure 4a). Moreover, GA treatment inhibited the expression of PPAR $\gamma$ 2 mRNA itself, suppressing a positive auto-regulatory loop. The respective PPAR $\gamma$  target mRNAs exhibited almost identical GA-concentration

dependence and IC50 values, which were close to that of PPAR $\gamma$  protein depletion (Supplementary Table S1). Hence, Hsp90 function is necessary for the transcriptional response of PPAR $\gamma$ , which creates and maintains the functional characteristics of mature adipocytes.<sup>19</sup>

Assessing the protein levels of PPAR $\gamma$  and the master adipokine adiponectin revealed their parallel decline in GA-treated mature adipocytes (Supplementary Figure S5). Hsp90 is generally a pro-survival protein,<sup>30</sup> and PPAR $\gamma$  has been reported to ensure the survival of mature adipocytes in mice.<sup>18</sup> Therefore, we investigated the impact of Hsp90 inhibition on the viability of differentiated 3T3-L1 cells. Significant cytotoxic effect was observed after a 48-h GA treatment, when a large

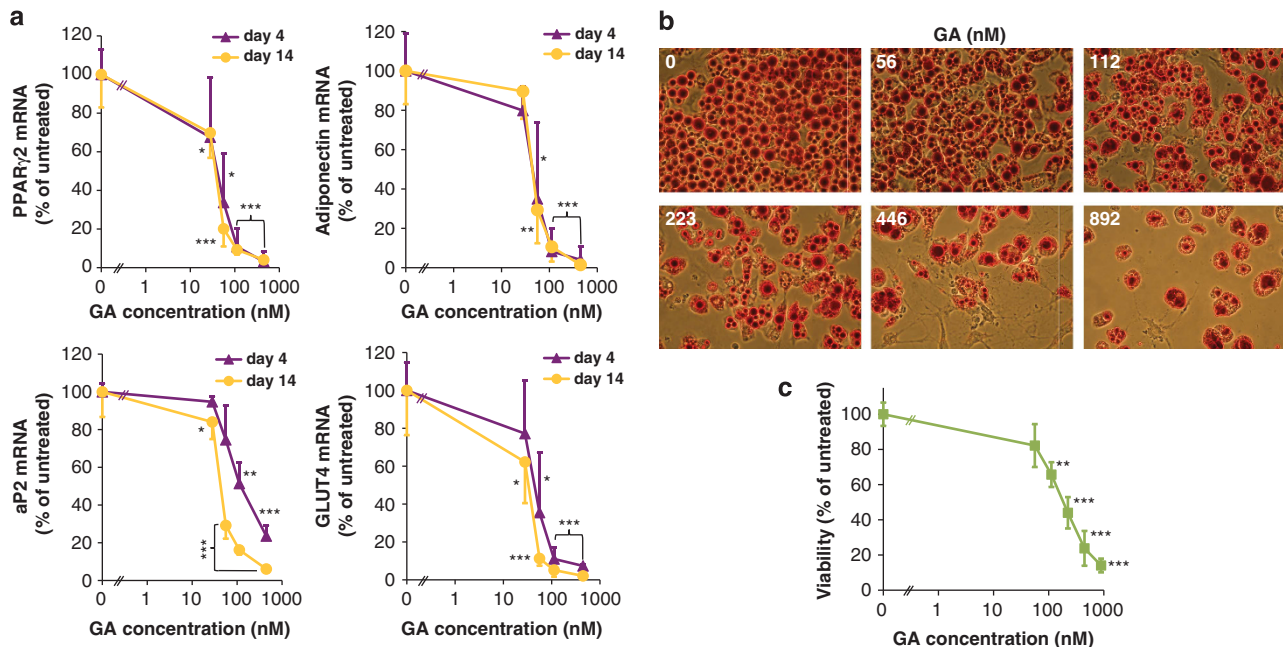


**Figure 4** GA inhibits the expression of PPAR $\gamma$  target genes and survival of mature adipocytes. (a) Effect of GA on PPAR $\gamma$ 2, adiponectin, GLUT4 and aP2 mRNA levels. mRNA expression data assayed by qRT-PCR from cells on day 4 and 14 treated by various concentrations of GA for 24 h on day 3 normalized to 28S rRNA and expressed relative to the respective (day 4 and day 14) untreated controls. IC<sub>50</sub> values are indicated in Supplementary Table S1. (b) Effect of GA on survival of differentiated adipocytes. Oil Red O staining of 3T3-L1 cells on day 14 treated by various concentrations of GA on day 12 for 48 h. Note the absence of Oil Red O negative cells. Images are representatives of three experiments. (c) Quantification of cell viability by trypan blue exclusion from the experiment shown in panel (b). Values in panels (a) and (c) are means  $\pm$  S.D. of three experiments and were statistically compared with the respective untreated controls. \* $P < 0.05$ , \*\* $P < 0.01$ , \*\*\* $P < 0.001$  by two-tailed unpaired *t*-test

number of mature adipocytes rounded up and died (Figures 4b and c). An  $\sim 2.5$ -fold longer treatment duration on day 12 produced a similar IC<sub>50</sub> value to the 20-h GA treatment on day 3 (170.2 *versus* 163.6 nM). Therefore, Hsp90 also ensures the survival of mature adipocytes.

#### Proteotoxic stress halts adipogenesis via abrogating the Hsp90-PPAR $\gamma$ complex.

Recent evidence confirmed that Hsp90 binds thermodynamically unstable proteins.<sup>25</sup> As an increasing amount of misfolded proteins may overload Hsp90 capacity, we investigated how proteotoxic stress interferes with PPAR $\gamma$  stability and adipogenesis. Strikingly, a transient moderate heat shock at 43°C employed on day 3 in differentiating 3T3-L1 cells induced a quantitative depletion of PPAR $\gamma$ , which was in contrast to the unchanged level of C/EBP $\alpha$  p42 (Figures 5a and b). As an underlying mechanism, the entire amount of PPAR $\gamma$  was rapidly misfolded and sedimented in the detergent-insoluble pellet, even if proteasome function was not pharmacologically inhibited (Figure 5c). This phenomenon was consistent with an increased load of the ubiquitin-proteasome system by heat-denatured substrates. In agreement with this, we were unable to immunoprecipitate PPAR $\gamma$  from the soluble fraction of heat-shocked lysates. However, Hsp90 largely preserved its solubility, indicating a loss of interaction with PPAR $\gamma$ . Under these conditions,  $\sim 50\%$  of Akt became insoluble (Figure 5c). The differential solubility of PPAR $\gamma$  and Akt paralleled their different sensitivity to Hsp90 inhibition (see Figures 2a and b), and suggests a stronger dependency of PPAR $\gamma$  on Hsp90 compared with Akt, and therefore its stronger aggregation in response to heat shock.

The transient folding defect of PPAR $\gamma$  in response to a moderate heat shock significantly inhibited PPAR $\gamma$ -dependent transcription, including a failure to increase its own mRNA expression by day 14 of adipocyte differentiation (Figure 5d). As a consequence, heat-shock treatment led to the cessation of adipocyte differentiation, while up to 120 min it did not largely interfere with cell survival (Figures 5e and f).

In physiological conditions,  $\sim 30\%$  of newly synthesized proteins are mistranslated, misfolded and degraded by the proteasome.<sup>37</sup> Therefore, we increased misfolded protein load by partial proteasome inhibition as an independent proteotoxic challenge. Indeed, a 20-h treatment with the proteasome inhibitor MG132 resulted in the destabilization of PPAR $\gamma$  (but not that of C/EBP $\alpha$  p42), inhibition of PPAR $\gamma$  target gene expression, as well as an impaired adipogenesis, similar to the effects observed after heat-shock and GA treatments (Supplementary Figures S6a–d).

#### Recovery from stress allows the continuation of adipogenic program by the restoration of PPAR $\gamma$ function.

The above observations demonstrated that different forms of global proteotoxic stress exert similar effects to pharmacological Hsp90 inhibition and abrogate all PPAR $\gamma$  folding, function and adipogenesis. To investigate whether adipocyte differentiation is reversibly restored upon attenuation of stress, after various doses of GA or heat-shock treatments on day 3, 3T3-L1 preadipocytes were re-exposed to the stimuli inducing differentiation on day 5 (Figure 6a). Cells were able to restore differentiation at a progressively decreasing level with increasing doses of GA and heat-

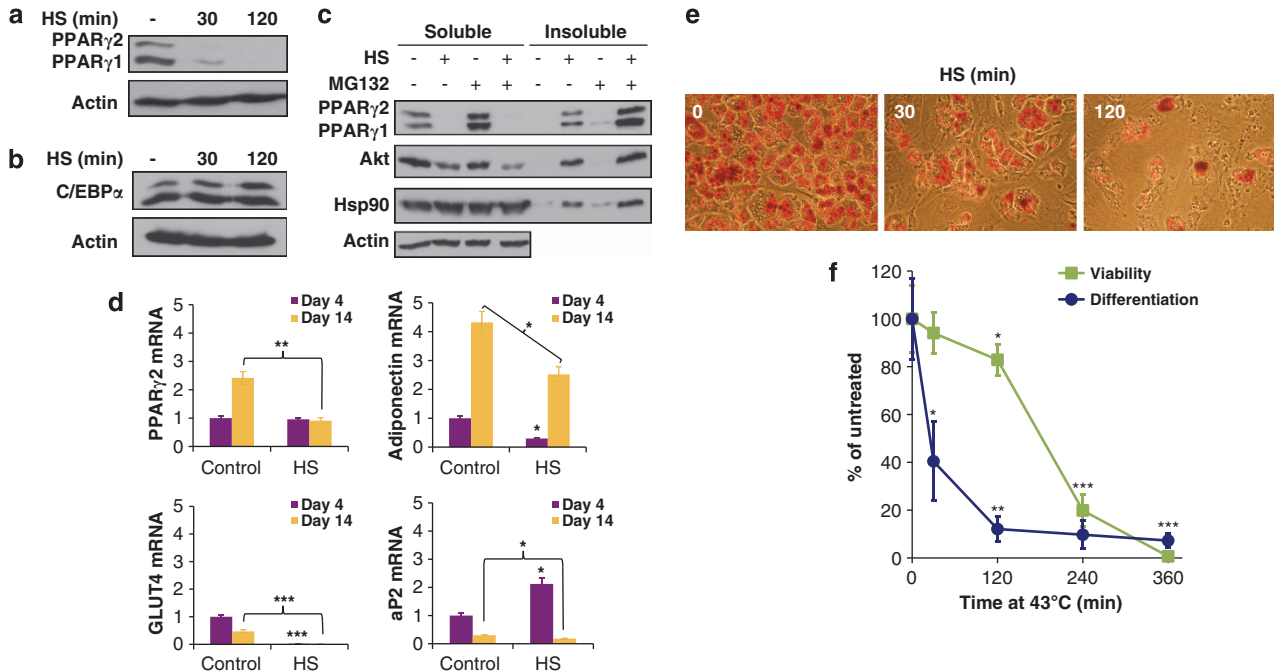


**Figure 5** Heat shock impairs PPAR $\gamma$  folding, transcriptional output and adipogenesis. Effect of heat shock on PPAR $\gamma$  (a) and on C/EBP $\alpha$  p42 (b) protein levels. Western blots of cells subjected to and lysed immediately after the indicated heat-shock (HS) treatments at 43 °C on day 3. (c) Heat-shock-induced misfolding and aggregation of PPAR $\gamma$ . Western blots of detergent soluble and insoluble lysates from cells treated by HS at 43 °C for 2 h and/or 20  $\mu$ M MG132 or DMSO vehicle for 4 h on day 3. (d) Effect of a 2-h HS at 43 °C on day 3 on PPAR $\gamma$ 2, adiponectin, GLUT4 and aP2 mRNA levels. mRNA expression data were assayed by qRT-PCR from cells on day 4 and 14, normalized to 28S rRNA and expressed relative to the untreated control. (e) Heat shock inhibits adipocyte differentiation. Oil Red O staining of differentiated cells on day 14 previously treated by HS at 43 °C for the indicated times on day 3. (f) Parallel quantification of Oil Red O absorption by photometry and cell viability by trypan blue exclusion on day 14. Images are representatives of three experiments. Values are means  $\pm$  S.D. of two (panel d) or three (panel f) experiments and were statistically compared with the respective untreated controls. \* $P$ <0.05, \*\* $P$ <0.01, \*\*\* $P$ <0.001 by two-tailed unpaired  $t$ -test

shock treatments (Supplementary Figures S7a–d). To assess the relationship between cell differentiation and PPAR $\gamma$  stability, we selected two conditions (112 nM GA and 2-h heat shock). Both treatments are characterized by maximal inhibition of differentiation and PPAR $\gamma$ , along with maximal preservation of viability to circumvent the influence of residual PPAR $\gamma$  activity and extensive cell death, respectively, on differentiation in response to the repeated stimulus. Re-exposure of cells to the differentiation medium led to a successful differentiation of the majority of the heat-shocked, but not GA-treated, cell population (Figure 6b), in line with the complete restoration of stabilized PPAR $\gamma$  protein levels after recovery from a transient heat shock, but not after GA treatment, respectively (Figure 6c). The slight appearance of PPAR $\gamma$  protein in GA-treated cells after the re-differentiation stimulus is consistent with the intracellular accumulation of, and sustained inhibition of Hsp90 by, GA (Figures 4a and 5d).<sup>30</sup> Neither intervention changed total Hsp90 protein level significantly (Figure 6c). These data suggest that recovery from stress allows the restoration of PPAR $\gamma$  stability and adipogenic function (Figure 6d).

## Discussion

Our study revealed a critical requirement of Hsp90 for the differentiation and survival of 3T3-L1 adipocytes and provided an underlying molecular mechanism by the identification of the master regulator PPAR $\gamma$  as an Hsp90 client. Both specific

Hsp90 inhibition and general proteotoxic stresses (heat-shock or proteasome inhibition) equally disrupted the Hsp90-PPAR $\gamma$  complex, destabilized PPAR $\gamma$  and halted adipogenesis. However, upon relief from stress, the differentiation program was continued by the restoration of PPAR $\gamma$  function.

The absolute requirement of Hsp90 for PPAR $\gamma$  stability and activity (Figures 2–4) is analogous with that of NR3 steroid receptors and many kinases<sup>23</sup> and indicates that PPAR $\gamma$  is a strong Hsp90 client, which appears unique among PPAR isoforms.<sup>28</sup> Systemic analysis of Hsp90-kinase interactions<sup>25</sup> and our data suggest that PPAR $\gamma$  harbors a level of conformational instability that makes it dependent on Hsp90. The discordant interaction of Hsp90 with PPARs<sup>28</sup> despite their  $\sim$ 80% sequence similarity may provide a tool to shed further light on the structural attributes that drive Hsp90/client recognition of nuclear receptors.

PPAR $\gamma$  is necessary and sufficient for adipogenesis<sup>14–16</sup> and is required for adipocyte survival in mice.<sup>18</sup> Our findings that GA treatment phenocopied PPAR $\gamma$  loss-of-function (Figures 1–4 and Supplementary Table S1) identifies the downregulation of PPAR $\gamma$  as an important downstream consequence of Hsp90 inhibition in adipocytes. Being an Hsp90 client creates an opportunity for regulation by a plethora of Hsp90-associated proteins. Indeed, the elegant evidence of such regulation, that a dephosphorylation of PPAR $\gamma$  at Ser-112 by the Hsp90 co-chaperone protein phosphatase 5 is indispensable for adipogenesis, has recently been published.<sup>38</sup> In addition to PPAR $\gamma$ , several



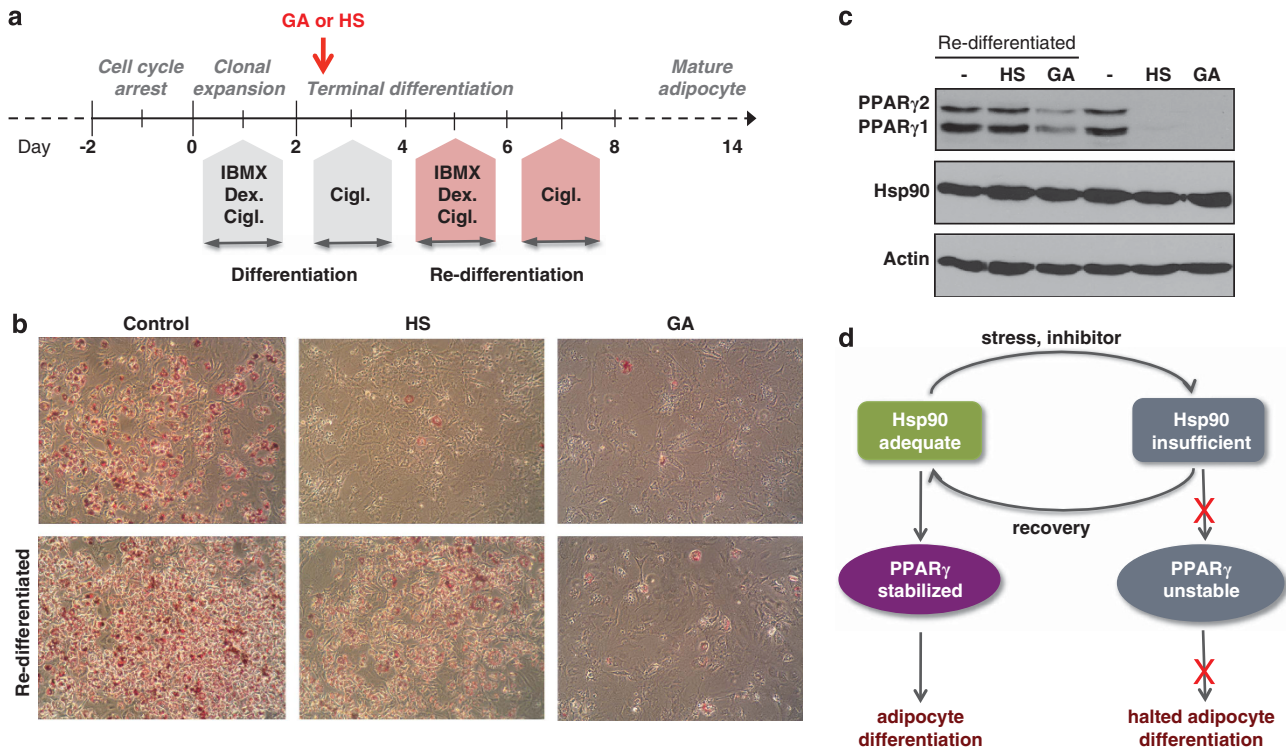


**Figure 6** Recovery from stress allows the continuation of adipogenic program by the restoration of PPAR $\gamma$  function. **(a)** Setup of the 3T3-L1 preadipocyte re-differentiation experiment. **(b)** Oil Red O staining of 3T3-L1 cells on day 14, treated by 112 nM GA for 24 h or by heat shock (HS) at 43°C for 2 h on day 3, with or without re-differentiation. **(c)** Effect of GA or HS at 43°C on day 3, followed or not by a re-differentiation, on PPAR $\gamma$  and Hsp90 protein levels on western blot. Images are representatives of three experiments. **(d)** Model of the stress-responsive regulation of PPAR $\gamma$  and adipogenesis. A reduction in Hsp90 availability by increase in unstable proteins or by pharmacologic inhibition leads to the release and destabilization of PPAR $\gamma$  (and other clients, such as Akt), which in turn compromises adipogenesis. A restoration of Hsp90 capacity by the attenuation of stress and adaptive proteostatic mechanisms resumes PPAR $\gamma$  stability and adipocyte differentiation. Note that the scheme depicts two extremes of a dynamic interactive process

pathways involving Hsp90 clients (including the insulin-dependent PI3K pathway, the mineralocorticoid receptor, as well as calcineurin and  $\beta$ -catenin in Wnt signaling) may contribute to Hsp90's effect on adipocyte differentiation and survival.<sup>36,39,40</sup> As an important example, we also observed a GA-induced depletion of Akt. In turn, adipose PPAR $\gamma$ 2 transgene induces Akt activation in mice, and insulin signaling promotes PPAR $\gamma$  activity.<sup>3,9</sup> Thus, GA may inhibit activatory crosstalks between insulin and PPAR $\gamma$  signaling. We suggest that the strong impact of Hsp90 inhibition beyond destabilizing individual clients also lies in affecting their interactions.

We observed prominent similarities of proteotoxic stresses (Figure 5 and Supplementary Figure S6) to pharmacologic Hsp90 inhibition. The stress-induced destabilization of the Hsp90 clients PPAR $\gamma$  and Akt suggests an increased load of Hsp90 by the expansion of the conformationally unstable pool of its clients resulting in its decreased support to PPAR $\gamma$  function and adipogenic signaling. Further experiments (Figure 6) showed that, upon cessation of stress, cells have the ability to restore the Hsp90-dependent support of adipogenesis. Pioneering studies from Susan Lindquist's group extended by others demonstrated that stresses burdening the Hsp90 buffer give rise to adaptive evolutionary changes.<sup>24,41–43</sup> However, what may be the benefit of the Hsp90-client interaction in the same generation? Our findings demonstrate that the interactions of Hsp90 with PPAR $\gamma$  and

Akt modulate cellular function and phenotype in a stress-responsive manner. We propose that Hsp90 provides a steady-state sensor, through which preadipocytes are able to immediately tune PPAR $\gamma$  activity, signaling and biological function with changing environmental conditions. Hsp90 is able to sense the ATP/ADP ratio, and ATP depletion *in vivo* has been reported to disrupt some Hsp90-client complexes.<sup>44,45</sup> Therefore, we hypothesize that PPAR $\gamma$  chaperoning might also be responsive to fluctuations in energy supply. Such a regulation may especially be useful in times of stress when fat mobilization fuels organismal adaptation.

An analogous stress-induced mechanism operates the heat-shock response through the dissociation of HSF1.<sup>31</sup> Similarly, reduction in Hsp90 level in HSF1/3-deficient cells mediates growth arrest upon heat shock by the destabilization of Cdc2.<sup>46</sup> We anticipate that the dynamic interactions with a diverse clientele may render Hsp90 a versatile stress-responsive modulator of complex biological responses.

In light of the increasing awareness that an optimal number of healthy adipocytes along with a robust PPAR $\gamma$  function are key to systemic health and lifespan,<sup>1,2,9,11</sup> our results may have broad therapeutic relevance. Accumulating evidence on a significant adipocyte turnover highlights adipogenesis as a therapeutic target in obesity.<sup>47,48</sup> Importantly, we found a much more potent inhibition of PPAR $\gamma$  by GA in adipocytes *versus* hepatoma cells (Figure 2 and Supplementary Figure S4),

which is reminiscent to the increased addiction of cancer cell clients to Hsp90.<sup>30</sup> Similarly, GA inhibited preadipocyte differentiation, preadipocyte survival and mature adipocyte survival, respectively, to progressively decreasing extent (Figures 1c and 4b). Hence, adipose Hsp90 inhibition might potently limit obesity by preventing adipocyte renewal and weight gain. However, considering the pivotal role of Hsp90 in various physiological processes in diverse tissues, further *in vivo* studies are needed to assess the feasibility of Hsp90 inhibition and the potential requirement of its adipose-specific targeting as a therapeutic strategy.

On the other hand, the vulnerability of the Hsp90-PPAR $\gamma$  interaction (Figures 2, 5 and 6) might limit PPAR $\gamma$  function and the response to thiazolidinediones in chronic distress, such as the metabolic syndrome.<sup>32</sup> Chaperone induction by different approaches, including a modest pharmacologic Hsp90 inhibition, has been widely shown to combat various age-related diseases.<sup>24,49</sup> Accordingly, these findings suggest that upregulation of the Hsp90 chaperone complex could strengthen adipocyte proteostasis and boost optimal PPAR $\gamma$ /client and adipose function. Such a possibility may gain support by the findings that chaperone induction either by systemic hyperthermia or by geranylgeranylacetone and BGP-15 drugs promote weight loss and/or improve insulin resistance in rodents and humans.<sup>50–54</sup> The involvement of adipose Hsp90 and PPAR $\gamma$  in these approaches, as well as the impact of adipose Hsp90/chaperone upregulation on systemic health, are exciting opportunities of further studies.

Our results on the GA-induced depletion of PPAR $\gamma$  in human hepatoma cells (Supplementary Figure S4) suggest that Hsp90 also stabilizes PPAR $\gamma$  in extra-adipose tissues. In addition to the TGF $\beta$  receptor,<sup>55</sup> PPAR $\gamma$  represents another anti-proliferative, differentiation-promoting Hsp90-client. Considering a dual, but primarily protective role of PPAR $\gamma$  in cancer,<sup>56</sup> it may be of interest to determine the efficacy of Hsp90 inhibition on tumor regression depending on the PPAR $\gamma$  background. Extra-adipose PPAR $\gamma$  in the liver, macrophages and brain modulates metabolism, inflammation, atherosclerosis and neuropathophysiology.<sup>3</sup> Therefore, the demonstration of a critical regulation of PPAR $\gamma$  by Hsp90 may open additional avenues of chaperone-related therapies in the treatment of various age-related diseases.

## Materials and Methods

**Materials.** Reagents for cell culture were from Gibco–Invitrogen (Carlsbad, CA, USA). Antibodies against PPAR $\gamma$  were from Abcam (Cambridge, UK) and from Cell Signaling Technology (Danvers, MA, USA). Anti-Akt, anti-C/EBP $\alpha$  and anti-adiponectin antibodies were from Cell Signaling Technology, and anti- $\beta$ -actin was from Sigma (St. Louis, MO, USA). Anti-Hsp90, Hsp90 $\alpha$  and Hsp90 $\beta$  antibodies were from Institute of Immunology Ltd. (Tokyo, Japan). Geldanamycin and novobiocin were from Sigma. The PI3K inhibitor LY294002 and the proteasome inhibitor MG132 were from Cell Signaling Technology and Calbiochem (San Diego, CA, USA), respectively. Complete protease inhibitor tablets were from Roche (Mannheim, Germany). Protein assay, electrophoresis and blotting reagents were from Bio-Rad (Hercules, CA, USA). The ECL kit was from Perkin-Elmer (Wellesley, MA, USA). All other reagents were from Sigma or Fluka (Buchs, Switzerland).

**Cell culture.** 3T3-L1 mouse fibroblasts and HepG2 human hepatoma cells were obtained from the ATCC. Both cell types were maintained in Dulbecco's modified Eagle medium (with 4.5 mg/ml glucose), supplemented with 2 mM L-glutamine, 1.5 g/l sodium bicarbonate, 4.5 g/l glucose, 100  $\mu$ g/ml streptomycin and 100 IU/ml

penicillin at isobaric oxygen in 5% CO $_2$  at 37 °C. 3T3-L1 and HepG2 cells were cultured in the presence of 10% bovine or 10% fetal bovine serum, respectively.

**Adipocyte differentiation and treatments.** 3T3-L1 cells were cultured to confluence. Differentiation was induced 2 days post-confluence (designated as day 0) by 1  $\mu$ M dexamethasone, 0.5 mM isobutylmethylxanthine and 1  $\mu$ M ciglitizone. After 48 h, cells were incubated with 1  $\mu$ M ciglitizone for 48 h. Subsequently, cells were maintained in DMEM supplemented with 10% fetal bovine serum till the end of the experiments. Cells were treated with various concentrations of geldanamycin, the PI3K inhibitor LY294002, heat-shock and/or the proteasome inhibitor MG132 as specified in the figure legends.

**Oil Red O staining and viability.** Cellular fat accumulation was monitored by Oil Red O staining on day 14 either visualized by microscopy or quantified by photometry. Oil Red O stock solution was prepared at 0.5% in isopropanol. Cells were cultured either on coverslips or in six-well plates, washed twice with PBS and fixed with 10% formalin in PBS for at least 1 h. After two washes in distilled water and 10 min incubation in 60% isopropanol, cells were stained for 10 min in Oil Red O solution freshly diluted into distilled water at a ratio of 3:2, followed by five washes in distilled water. Coverslips were mounted using Vectashield (Vector Laboratories, Burlingame, CA, USA) visualized and imaged by a Nikon Eclipse E400 microscope/camera. Plates were observed using an Alpha XD2-2T inverted microscope and photographed by an Alpha DMC-510 USB camera. For photometry cells were allowed to dry, and Oil Red O was eluted by isopropanol for 10 min. Optical density was measured at 500 nm by a Thermo Varioskan Flash photometer (Thermo Scientific, Wiesbaden, Germany) using isopropanol as blank. In order to directly compare cell survival with differentiation, parallel samples from the same experiments were assayed on the same day both for triglyceride accumulation by Oil Red O incorporation and for viability by trypan blue exclusion.

**Cell lysis, purification of aggregates and western blotting.** After treatments, cells were lysed on ice with WB lysis buffer (50 mM Tris, 300 mM NaCl, 1 mM MgCl $_2$ , 0.5 mM EDTA, 0.1 mM EGTA, 20% glycerol, 1% NP40, 0.5 mM DTT, 2  $\times$  Complete, pH 7.6) for 20 min at 4 °C, vigorously vortexed, and centrifuged at 13 000 r.p.m. for 10 min in a microcentrifuge. Protein concentration of the supernatants was determined by Bradford method, and equal amounts of proteins were subjected to SDS-PAGE. The aggregation of PPAR $\gamma$  was assessed as previously described.<sup>57</sup> Briefly, detergent-insoluble pellets, containing aggregated proteins, were solubilized in urea buffer (2% SDS, 6 M urea, 30 mM Tris, pH 7.6). Equal volumes of protein extracts from each fraction were resolved by SDS-PAGE. Western blotting was performed by transfer to nitrocellulose membrane and by blocking in 5% (w/v) skim milk powder. Blots were probed with the appropriate primary antibodies overnight at 4 °C and incubated with peroxidase-conjugated secondary antibodies for an hour at room temperature and developed using ECL detection. The protein levels were determined by densitometric analysis of the western blots using the Image J (NIH, Bethesda, MD, USA) and normalized to the corresponding  $\beta$ -actin level.

**mRNA expression analysis.** mRNA was prepared and was reverse transcribed using the GeneJET RNA Purification Kit and the RevertAid<sup>TM</sup> cDNA Synthesis Kit, respectively (Fermentas, Vilnius, Lithuania). Sequences of primer sets for mouse PPAR $\gamma$ 2, adiponectin, GLUT4, aP2 and 28S rRNA were described elsewhere.<sup>58</sup> Quantitative PCR was performed in an ABI 7300 System by using Maxima SYBR Green/ROX qPCR Master Mix (Fermentas) according to the manufacturer's instructions. Relative amounts of mRNA were determined using the Comparative CT Method for quantification and were normalized to 28S rRNA levels.

**Immunoprecipitation.** 5  $\times$  10<sup>6</sup> cells were treated by 0.25  $\mu$ g/ml geldanamycin or DMSO for 2 h. Then, cells were washed three times and scraped in ice-cold PBS. Lysis was performed in IP lysis buffer (50 mM Tris, 2 mM EDTA, 100 mM NaCl, 1 mM Na $_3$ VO $_4$ , 1% NP40, 2 $\times$  Complete). PPAR $\gamma$  was immunoprecipitated by a monoclonal anti-PPAR $\gamma$  antibody. Pellets were washed five times with lysis buffer and analyzed by SDS-PAGE and immunoblotting with anti-Hsp90 and anti-PPAR $\gamma$  antibodies.

**Statistical analysis.** Data were compared by two-tailed unpaired *t*-test. Variables were expressed as mean  $\pm$  standard deviation (s.d). Statistical significance was indicated as follows: \**P* < 0.05, \*\**P* < 0.01, \*\*\**P* < 0.001.



## Conflict of Interest

The authors declare no conflict of interest.

**Acknowledgements.** We thank Lívius Wunderlich and Péter Szélenyi for reagents, Zsolt Rónai for help in qPCR experiments and Beatrix Gilányi for technical help. We are grateful to members of the Söti Group, and the Editor and anonymous reviewers of this manuscript for helpful comments and suggestions. This work was supported by grants from the EU (FP6-518230, TÁMOP-4.2.2/B-10/1-2010-0013), a joint grant of the Hungarian Science Foundation and Norway Grants (NNF-78794), the Hungarian Science Foundation (OTKA K69105 and OTKA-K83314). During the completion of this study, C.S. was a Bolyai Research Scholar of the Hungarian Academy of Sciences.

## Author Contributions

CS and MTN conceived and designed the experiments. MTN performed the experiments. MTN and CS analyzed the data. CS, PC and MTN wrote the manuscript.

- Rosen ED, Spiegelman BM. Adipocytes as regulators of energy balance and glucose homeostasis. *Nature* 2006; **444**: 847–853.
- Lefterova MI, Lazar MA. New developments in adipogenesis. *Trends Endocrinol Metab* 2009; **20**: 107–114.
- Tontonoz P, Spiegelman BM. Fat and beyond: the diverse biology of PPAR $\gamma$ . *Annu Rev Biochem* 2008; **77**: 289–312.
- Christodoulides C, Vidal-Puig A. PPARs and adipocyte function. *Mol Cell Endocrinol* 2010; **318**: 61–68.
- Duan SZ, Ivashchenko CY, Whitesall SE, D'Alecy LG, Duquaine DC, Brosius FC 3rd et al. Hypotension, lipodystrophy, and insulin resistance in generalized PPAR $\gamma$ -deficient mice rescued from embryonic lethality. *J Clin Invest* 2007; **117**: 812–822.
- He W, Barak Y, Hevener A, Olson P, Liao D, Le J et al. Adipose-specific peroxisome proliferator-activated receptor gamma knockout causes insulin resistance in fat and liver but not in muscle. *Proc Natl Acad Sci USA* 2003; **100**: 15712–15717.
- Medina-Gomez G, Gray SL, Yetukuri L, Shimomura K, Virtue S, Campbell M et al. PPAR gamma 2 prevents lipotoxicity by controlling adipose tissue expandability and peripheral lipid metabolism. *PLoS Genet* 2007; **3**: e64.
- Agostini M, Schoenmakers E, Mitchell C, Szatmari I, Savage D, Smith A et al. Non-DNA binding, dominant-negative, human PPAR $\gamma$  mutations cause lipodystrophic insulin resistance. *Cell Metab* 2006; **4**: 303–311.
- Sugii S, Olson P, Sears DD, Saberi M, Atkins AR, Barish GD et al. PPAR $\gamma$  activation in adipocytes is sufficient for systemic insulin sensitization. *Proc Natl Acad Sci USA* 2009; **106**: 22504–22509.
- Deeb SS, Fajas L, Nemoto M, Pihlajamaki J, Mykkanen L, Kuusisto J et al. A Pro12Ala substitution in PPAR $\gamma$ 2 associated with decreased receptor activity, lower body mass index and improved insulin sensitivity. *Nat Genet* 1998; **20**: 284–287.
- Argmann C, Dobrin R, Heikkinen S, Auburtin A, Pouilly L, Cock TA et al. Ppargamma2 is a key driver of longevity in the mouse. *PLoS Genet* 2009; **5**: e1000752.
- Heikkinen S, Argmann C, Feige JN, Koutnikova H, Champy MF, Dali-Youcef N et al. The Pro12Ala PPAR $\gamma$ 2 variant determines metabolism at the gene-environment interface. *Cell Metab* 2009; **9**: 88–98.
- Wu Z, Bucher NL, Farmer SR. Induction of peroxisome proliferator-activated receptor gamma during the conversion of 3T3 fibroblasts into adipocytes is mediated by C/EBP $\beta$ , C/EBP $\delta$ , and glucocorticoids. *Mol Cell Biol* 1996; **16**: 4128–4136.
- Kubota N, Terauchi Y, Miki H, Tamemoto H, Yamauchi T, Kameda K et al. PPAR gamma mediates high-fat diet-induced adipocyte hypertrophy and insulin resistance. *Mol Cell* 1999; **4**: 597–609.
- Rosen ED, Sarraf P, Troy AE, Bradwin G, Moore K, Milstone DS et al. PPAR gamma is required for the differentiation of adipose tissue in vivo and in vitro. *Mol Cell* 1999; **4**: 611–617.
- Rosen ED, Hsu CH, Wang X, Sakai S, Frezman MW, Gonzalez FJ et al. C/EBP $\alpha$  induces adipogenesis through PPAR $\gamma$ : a unified pathway. *Genes Dev* 2002; **16**: 22–26.
- Lefterova MI, Zhang Y, Steger DJ, Schupp M, Schug J, Cristancho A et al. PPAR $\gamma$  and C/EBP factors orchestrate adipocyte biology via adjacent binding on a genome-wide scale. *Genes Dev* 2008; **22**: 2941–2952.
- Imai T, Takakuwa R, Marchand S, Dentz E, Bornert JM, Messaddeq N et al. Peroxisome proliferator-activated receptor gamma is required in mature white and brown adipocytes for their survival in the mouse. *Proc Natl Acad Sci USA* 2004; **101**: 4543–4547.
- Tamori Y, Masugi J, Nishino N, Kasuga M. Role of peroxisome proliferator-activated receptor-gamma in maintenance of the characteristics of mature 3T3-L1 adipocytes. *Diabetes* 2002; **51**: 2045–2055.
- Floyd ZE, Stephens JM. Interferon-gamma-mediated activation and ubiquitin-proteasome-dependent degradation of PPAR $\gamma$  in adipocytes. *J Biol Chem* 2002; **277**: 4062–4068.
- Hauser S, Adelmant G, Sarraf P, Wright HM, Mueller E, Spiegelman BM. Degradation of the peroxisome proliferator-activated receptor gamma is linked to ligand-dependent activation. *J Biol Chem* 2000; **275**: 18527–18533.
- van Beekum O, Fleskens V, Kalkhoven E. Posttranslational modifications of PPAR-gamma: fine-tuning the metabolic master regulator. *Obesity (Silver Spring)* 2009; **17**: 213–219.
- Pratt WB, Toft DO. Regulation of signaling protein function and trafficking by the hsp90/hsp70-based chaperone machinery. *Exp Biol Med (Maywood)* 2003; **228**: 111–133.
- Taipale M, Jarosz DF, Lindquist S. HSP90 at the hub of protein homeostasis: emerging mechanistic insights. *Nat Rev Mol Cell Biol* 2010; **11**: 515–528.
- Taipale M, Krykbaeva I, Koeva M, Kayatekin C, Westover KD, Karras GI et al. Quantitative analysis of hsp90-client interactions reveals principles of substrate recognition. *Cell* 2012; **150**: 987–1001.
- Denis M, Cuthill S, Wikstrom AC, Poellinger L, Gustafsson JA. Association of the dioxin receptor with the Mr 90,000 heat shock protein: a structural kinship with the glucocorticoid receptor. *Biochem Biophys Res Commun* 1988; **155**: 801–807.
- Dalman FC, Koenig RJ, Perdew GH, Massa E, Pratt WB. In contrast to the glucocorticoid receptor, the thyroid hormone receptor is translated in the DNA binding state and is not associated with hsp90. *J Biol Chem* 1990; **265**: 3615–3618.
- Sumanasekera WK, Tien ES, Davis JW 2nd, Turpey R, Perdew GH, Vanden Heuvel JP. Heat shock protein-90 (Hsp90) acts as a repressor of peroxisome proliferator-activated receptor-alpha (PPARalpha) and PPARbeta activity. *Biochemistry* 2003; **42**: 10726–10735.
- Whitesell L, Mimnaugh EG, De Costa B, Myers CE, Neckers LM. Inhibition of heat shock protein HSP90-pp60v-src heteroprotein complex formation by benzoquinone ansamycins: essential role for stress proteins in oncogenic transformation. *Proc Natl Acad Sci USA* 1994; **91**: 8324–8328.
- Neckers L, Workman P. Hsp90 molecular chaperone inhibitors: are we there yet? *Clin Cancer Res* 2012; **18**: 64–76.
- Zou J, Guo Y, Guettouche T, Smith DF, Voellmy R. Repression of heat shock transcription factor HSF1 activation by HSP90 (HSP90 complex) that forms a stress-sensitive complex with HSF1. *Cell* 1998; **94**: 471–480.
- Dancso B, Spiro Z, Arslan MA, Nguyen MT, Papp D, Csermely P et al. The heat shock connection of metabolic stress and dietary restriction. *Curr Pharm Biotechnol* 2010; **11**: 139–145.
- Armani A, Mammi C, Marzolla V, Calanchini M, Antelmi A, Rosano GM et al. Cellular models for understanding adipogenesis, adipose dysfunction, and obesity. *J Cell Biochem* 2010; **110**: 564–572.
- Marcu MG, Schulte TW, Neckers L. Novobiocin and related coumarins and depletion of heat shock protein 90-dependent signaling proteins. *J Natl Cancer Inst* 2000; **92**: 242–248.
- Basso AD, Solit DB, Chiosis G, Giri B, Tschisler P, Rosen N. Akt forms an intracellular complex with heat shock protein 90 (Hsp90) and Cdc37 and is destabilized by inhibitors of Hsp90 function. *J Biol Chem* 2002; **277**: 39858–39866.
- Sakaue H, Ogawa W, Matsumoto M, Kuroda S, Takata M, Sugimoto T et al. Posttranscriptional control of adipocyte differentiation through activation of phosphoinositide 3-kinase. *J Biol Chem* 1998; **273**: 28945–28952.
- Schubert U, Anton LC, Gibbs J, Norbury CC, Yewdell JW, Bannink JR. Rapid degradation of a large fraction of newly synthesized proteins by proteasomes. *Nature* 2000; **404**: 770–774.
- Hinds TD Jr, Stechschulte LA, Cash HA, Whisler D, Banerjee A, Yong W et al. Protein phosphatase 5 mediates lipid metabolism through reciprocal control of glucocorticoid receptor and peroxisome proliferator-activated receptor-gamma (PPARgamma). *J Biol Chem* 2011; **286**: 42911–42922.
- Caprio M, Feve B, Claes A, Viengchareun S, Lombes M, Zennaro MC. Pivotal role of the mineralocorticoid receptor in corticosteroid-induced adipogenesis. *FASEB J* 2007; **21**: 2185–2194.
- Kennell JA, MacDougald OA. Wnt signaling inhibits adipogenesis through beta-catenin-dependent and -independent mechanisms. *J Biol Chem* 2005; **280**: 24004–24010.
- Jarosz DF, Lindquist S. Hsp90 and environmental stress transform the adaptive value of natural genetic variation. *Science* 2010; **330**: 1820–1824.
- Specchia V, Piacentini L, Tritto P, Fanti L, D'Alessandro R, Palumbo G et al. Hsp90 prevents phenotypic variation by suppressing the mutagenic activity of transposons. *Nature* 2010; **463**: 662–665.
- Chen G, Bradford WD, Seidel CW, Li R. Hsp90 stress potentiates rapid cellular adaptation through induction of aneuploidy. *Nature* 2012; **482**: 246–250.
- Peng X, Guo X, Borkan SC, Bharti A, Kuramochi Y, Calderwood S et al. Heat shock protein 90 stabilization of ErbB2 expression is disrupted by ATP depletion in myocytes. *J Biol Chem* 2005; **280**: 13148–13152.
- Hu LM, Bodwell J, Hu JM, Ori E, Munck A. Glucocorticoid receptors in ATP-depleted cells. Dephosphorylation, loss of hormone binding, HSP90 dissociation, and ATP-dependent cycling. *J Biol Chem* 1994; **269**: 6571–6577.
- Nakai A, Ishikawa T. Cell cycle transition under stress conditions controlled by vertebrate heat shock factors. *EMBO J* 2001; **20**: 2885–2895.
- Spalding KL, Amer E, Westermark PO, Bernard S, Buchholz BA, Bergmann O et al. Dynamics of fat cell turnover in humans. *Nature* 2008; **453**: 783–787.

48. Strawford A, Antelo F, Christiansen M, Hellerstein MK. Adipose tissue triglyceride turnover, de novo lipogenesis, and cell proliferation in humans measured with  $2H_2O$ . *Am J Physiol Endocrinol Metab* 2004; **286**: E577–E588.
49. Powers ET, Morimoto RI, Dillin A, Kelly JW, Balch WE. Biological and chemical approaches to diseases of proteostasis deficiency. *Annu Rev Biochem* 2009; **78**: 959–991.
50. Kokura S, Adachi S, Manabe E, Mizushima K, Hattori T, Okuda T *et al*. Whole body hyperthermia improves obesity-induced insulin resistance in diabetic mice. *Int J Hyperthermia* 2007; **23**: 259–265.
51. Gupte AA, Bomhoff GL, Swerdlow RH, Geiger PC. Heat treatment improves glucose tolerance and prevents skeletal muscle insulin resistance in rats fed a high-fat diet. *Diabetes* 2009; **58**: 567–578.
52. Adachi H, Kondo T, Ogawa R, Sasaki K, Morino-Koga S, Sakakida M *et al*. An acyclic polyisoprenoid derivative, geranylgeranylacetone protects against visceral adiposity and insulin resistance in high-fat-fed mice. *Am J Physiol Endocrinol Metab* 2010; **299**: E764–E771.
53. Chung J, Nguyen AK, Henstridge DC, Holmes AG, Chan MH, Mesa JL *et al*. HSP72 protects against obesity-induced insulin resistance. *Proc Natl Acad Sci USA* 2008; **105**: 1739–1744.
54. Literati-Nagy B, Kulcsar E, Literati-Nagy Z, Buday B, Peterfai E, Horvath T *et al*. Improvement of insulin sensitivity by a novel drug, BGP-15, in insulin-resistant patients: a proof of concept randomized double-blind clinical trial. *Horm Metab Res* 2009; **41**: 374–380.
55. Wrighton KH, Lin X, Feng XH. Critical regulation of TGF $\beta$  signaling by Hsp90. *Proc Natl Acad Sci USA* 2008; **105**: 9244–9249.
56. Peters JM, Shah YM, Gonzalez FJ. The role of peroxisome proliferator-activated receptors in carcinogenesis and chemoprevention. *Nat Rev Cancer* 2012; **12**: 181–195.
57. Arslan MA, Chikina M, Csermely P, Soti C. Misfolded proteins inhibit proliferation and promote stress-induced death in SV40-transformed mammalian cells. *FASEB J* 2012; **26**: 766–777.
58. Ezure T, Amano S. Heat stimulation reduces early adipogenesis in 3T3-L1 preadipocytes. *Endocrine* 2009; **35**: 402–408.

Supplementary Information accompanies this paper on Cell Death and Differentiation website (<http://www.nature.com/cdd>)